

Aggregated Packet Transmission in Duty-Cycled WSNs: Modeling and Performance Evaluation

Lakshmikanth Guntupalli, *Student Member, IEEE*, Jorge Martinez-Bauset, Frank Y. Li, *Senior Member, IEEE*, and Mary Ann Weitnauer, *Senior Member, IEEE*

Abstract—Duty cycling (DC) is a popular technique for energy conservation in wireless sensor networks that allows nodes to wake up and sleep periodically. Typically, a single packet transmission (SPT) occurs per cycle, leading to possibly long delay. With aggregated packet transmission (APT), nodes transmit a batch of packets in a single cycle. The potential benefits brought by an APT scheme include shorter delay, higher throughput and higher energy efficiency. In the literature, different analytical models have been proposed to evaluate the performance of SPT schemes. However, no analytical models for the APT mode on synchronous DC medium access control mechanisms exist. In this paper, we first develop a three-dimensional (3D) discrete time Markov chain (DTMC) model to evaluate the performance of an APT scheme with packet retransmission enabled. The proposed model captures the dynamics of the state of the queue of nodes and the retransmission status, as well as the evolution of the number of active nodes in the network, i.e., nodes with a non-empty queue. We then study the number of retransmissions needed to transmit a packet successfully. Based on the observations, we develop another less complex DTMC model with infinite retransmissions which embodies only two dimensions. Furthermore, we extend the 3D model into a four-dimensional model by considering error-prone channel conditions. The proposed models are adopted to determine packet delay, throughput, packet loss, energy consumption, and energy efficiency. Furthermore the analytical models are validated through discrete-event based simulations. Numerical results show that an APT scheme achieves substantially better performance than its SPT counterpart in terms of delay, throughput, packet loss and energy efficiency, and that the developed analytical models reveal precisely the behavior of the APT scheme.

Index Terms—Duty-cycled wireless sensor networks, discrete time Markov chain model, packet aggregation, performance evaluation.

Copyright (c) 2015 IEEE. Personal use of this material is permitted. However, permission to use this material for any other purposes must be obtained from the IEEE by sending a request to pubs-permissions@ieee.org.

Manuscript received July 1, 2015; revised November 8, 2015; accepted December 21, 2015. The research leading to these results has received funding from the EU FP7-PEOPLE-IRSES program under grant agreement 247083, project acronym S2EuNet. This work was partially performed while Lakshmikanth Guntupalli was visiting the School of Electrical and Computer Engineering, Georgia Institute of Technology. The research of Jorge Martinez-Bauset was partially supported by the Ministry of Economy and Competitiveness of Spain under grant TIN2013-47272-C2-1-R. The research of Mary Ann Weitnauer was partially supported by the National Science Foundation grant CNS-1017984. The review of this paper was coordinated by Prof. Y. Qian.

Lakshmikanth Guntupalli and Frank Y. Li are with the Dept. of Information and Communication Technology, University of Agder (UiA), N-4898 Grimstad, Norway (Email: {lakshmikanth.guntupalli; frank.li}@uia.no).

Jorge Martinez-Bauset is with the Dept. of Communications, Universitat Politècnica de València (UPV), ETSIT, Camino de Vera s/n, 46022 València, Spain (Email: jmartinez@upv.es).

Mary Ann Weitnauer is with the School of Electrical and Computer Engineering, Georgia Institute of Technology, Atlanta, GA 30332-0250, USA (Email: mary.ann.weitnauer@ece.gatech.edu).

I. INTRODUCTION

ONE of the goals for designing medium access control (MAC) protocols in energy constrained wireless sensor networks (WSNs) is to achieve higher energy efficiency. Among the proposed energy efficient techniques, duty cycling (DC) is employed in many existing MAC protocols. By following DC, nodes turn their radios *on* and *off* periodically to avoid idle listening in order to save energy consumption. Sensor-MAC (S-MAC) [1] is a benchmark example for synchronous DC MAC protocols. In S-MAC, nodes transmit or receive only one DATA packet per cycle. This transmission scheme is referred to hereafter as single packet transmission (SPT). Since only one packet is transmitted per cycle, packets stored in the queue might need to wait a long time before being delivered. On the other hand, in many WSN applications, timely data delivery is required for event-driven scenarios. For example, in fire detection scenarios, alarms should be alerted in real-time so that urgent actions can take place prior to the occurrence of a disaster. Furthermore, an appropriate decision can be taken when accurate data is available and better accuracy can be achieved with higher data rate.

In order to boost data rate and minimize delay in WSNs, packet aggregation, in which a batch of packets are transmitted together, has been proposed as a pragmatic approach. Packet aggregation is a feasible technique for WSNs since all packets are typically addressed to one node, i.e., the sink node [2]. Aggregated data transmission helps to increase the probability that a node transmits a packet successfully, since queues are emptied faster when multiple packets are transmitted together, and correspondingly the mean number of contending nodes per cycle decreases [3]. Packet aggregation may also bring other benefits like shorter delay and higher energy efficiency. Indeed, many data aggregation schemes have been proposed for the purpose of energy saving, delay reduction, collision avoidance, or more accurate data transmission [4]. However, very few analytical models exist for performance evaluation of aggregated data transmission in WSNs.

In this paper, we adopt the concept of packet aggregation and propose an analytical model to evaluate the performance of an aggregated packet transmission (APT) scheme. This scheme operates in WSNs with a synchronous DC MAC protocol like S-MAC. We refer to the set of consecutive packets in the buffer of a node that will be transmitted together in the same cycle as a *frame*. The maximum number of packets aggregated in a frame is constrained by the maximum frame length of the wireless link, as well as the number of packets in the queue.

We develop first a three-dimensional (3D) discrete-time Markov chain (DTMC) to model the time evolution of the state of a node in a WSN, where nodes have finite queue capacity and operate according to S-MAC. One of the three state elements is dedicated to track the number of retransmissions experienced by the frame at the head of the queue of the node. We analyze accordingly the number of retransmissions required to successfully transmit a frame in an error-free channel, where losses only occur due to collisions in the channel. Based on the results of the 3D DTMC, we observe that, in many configurations, 99.999% of the frames are successfully delivered after at most two retransmissions. Therefore, by configuring the maximum retransmission counter in the nodes to two or larger, we might achieve zero or close-to-zero packet loss. Correspondingly, we propose a simpler two-dimensional (2D) DTMC model that allows infinite retransmissions to evaluate the performance of the APT scheme. Clearly, the state of a node in this model omits the element dedicated to retransmissions. We observe that this model is applicable to many realistic scenarios where initial packet transmission failures are finally recovered by retransmissions.

On the other hand, although the error-free channel assumption has been extensively adopted in the literature [5], [6], [7], it is more realistic to consider that wireless channels are intrinsically error-prone. Accordingly, we further develop a four-dimensional (4D) model by defining multiple *loss* and *non-loss* states to characterize error-prone wireless channels, and integrate them into the the 3D model. This modeling approach captures both first- and second-order statistics with sufficient accuracy, which is considered an adequate characterization of the wireless link for practical scenarios. Using the proposed models, different performance parameters are studied, like average packet delay, throughput, average energy consumption per cycle, and energy efficiency.

The rest of this paper is structured as follows. Section II reviews the related work and Section III describes the network model. In Section IV, we present both the 3D and 2D DTMC models in details. The expressions for performance parameters are deduced in Section V. The performance of the APT and SPT schemes is compared in Section VI. Furthermore, the 4D model is presented in Section VII, before the paper is concluded in Section VIII.

II. RELATED WORK AND CONTRIBUTIONS

Among the analytical models proposed to analyze the performance of carrier sense multiple access with collision avoidance (CSMA/CA) MAC protocols, the model proposed in [5] is a popular one. It is based on a DTMC that captures the behavior of an individual node contending for channel access. The primary assumptions of the model are: *error-free channel*, the collision probability of a station when it attempts to transmit is independent of its state, and nodes operate in the saturation mode. These assumptions make the model simple, yet quite accurate. Since then, Bianchi's model has been extensively studied, refined and extended to different scenarios. See for example [8] and their references.

Most of the models based on Bianchi's approach do not keep track of the number of packets in the queue of the node, and

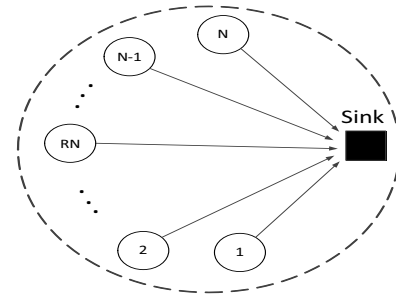


Fig. 1. A network model where all nodes are reachable within one hop and send DATA frames to a single sink.

therefore they cannot be applied to an APT MAC mechanism like the one studied here. When a node employing APT wins access to the medium, the number of packets in the queue must be known to define the size of the frame. If this information is not known, the time evolution of the system cannot be modeled with precision.

Exceptions exist. For example, the 3D DTMC model proposed in [6] extends the model in [5] with a new dimension to keep track of the state of the queue. However, there is another important reason that makes previous models not directly applicable for evaluating the performance of synchronous DC MAC protocols like S-MAC, since the backoff timers designed therein are reset at each cycle [7].

A continuous time Markov chain (CTMC) with exponentially distributed times in the *active* and *sleep* states was developed to model the behavior of sensor nodes with finite queue capacity in [9]. Clearly when nodes have random cycle duration, the synchronization of node schedules becomes a tedious and energy consuming task. Another model for analyzing S-MAC was proposed in [10], based on an $M/G/1$ model. However, it requires that packet arrivals follow a Poisson process and that each node has an infinite buffer.

Provided the synchronous nature of S-MAC, modeling S-MAC based WSNs using a DTMC seems to be a natural option. To model the evolution with time of the state of a generic node in the network, a one-dimensional (1D) DTMC model supporting a general packet arrival distribution per cycle, finite queue and zero packet retransmissions was proposed in [7]. The same authors proposed in [11] a 2D model to analyze the impact of packet retransmissions. However, the models in [7] and [11] were developed based on the assumption that the probability that a node is active is independent of the other nodes being active. Nodes are active, and contend for channel access, if their queues are non-empty.

We argue that some degree of dependence occurs among nodes in practice. This is because the probability of successful transmission of a node depends on the number of active nodes in the network, and this number varies over time depending on the state of the other nodes. For a WSN employing S-MAC, we compared in [12] a model that considers nodes as mutually independent with another model that incorporates the dependence among nodes. The study concludes that substantially more accurate results can be obtained when dependence is incorporated into the model.

In this paper, we propose a 3D DTMC that incorporates the dependency among nodes in the network. To clarify the difference between our model and the previous models, let (i) be the state of the 1D DTMC studied in [7], where i is the number of packets found at the queue of a node. Also, let (i, r) be the state of the previous 2D DTMCs [11], [13], where i has the same definition and r is the number of retransmissions experienced by the packet at the head of the queue of the node. In contrast, the state of the proposed 3D DTMC is defined by a triplet (i, k, r) , where k keeps track of the number of *active* nodes in the network. The state of our 2D DTMC is defined by (i, k) , where the r element has been omitted, and it is therefore different from the previous 2D DTMCs in [11], [13]. It is furthermore worth mentioning that all aforementioned models were developed for the SPT scheme without considering packet aggregation.

When data is sensed by a group of neighboring nodes, it tends to be somewhat space-correlated and redundant. Then unprocessed transmission of such data is likely to waste energy and degrade network performance. Correspondingly, packet aggregation in WSNs has been proposed, mainly from a routing perspective [14], [15], [16], [17], [18]. That is, cluster-heads perform the processing and aggregation of intra-cluster and inter-cluster information, before it is forwarded towards the sink. For example in [16] the authors obtained an approximated closed-form expression for end-to-end delay when data aggregation was enabled in a generic multi-hop WSN. Nonetheless, the above aggregation schemes for WSNs do not consider any specific MAC layer protocol.

Currently, there exist only a few MAC protocols that integrate data aggregation in WSNs. Among them, aggregation MAC (AG-MAC) [19] is a synchronous DC MAC protocol. A joint aggregation and MAC (JAM) [20] scheme was proposed for RI-MAC [21] as another asynchronous DC MAC protocol. Moreover, a lifetime balanced data aggregation scheme was proposed for DC WSNs in [22]. However, these studies have been carried out largely by simulations or test-bed based experiments.

In this paper, we aim at modeling analytically the performance of packet aggregation at the MAC layer and the intra-cluster level. To the best of our knowledge, this paper is the first attempt to develop analytical models for MAC level packet aggregation in synchronous duty-cycled WSNs. In summary, the main contributions of this paper are as follows:

- We propose a novel modeling approach to evaluate the performance of an aggregated packet transmission scheme that operates in WSNs with finite capacity queue running on a synchronous DC MAC protocol like S-MAC. A salient feature of the proposed analytical model is that it handles the dependence that occurs among nodes in practice by keeping track of the number of active nodes in the network. This makes the proposed model substantially more accurate than the other models that assume mutual independence among nodes [12].
- A 3D DTMC is proposed to model the time evolution of the state of a node with finite retransmissions. To reduce the complexity of the 3D DTMC, a less complex 2D DTMC allowing infinite retransmissions is developed as

an alternative model for scenarios where a vast majority of frames that arrive with error can be recovered by re-transmissions. In addition to the 2D and 3D models which are built based on an error-free channel assumption, a 4D model which integrates error-prone channel conditions into the 3D model is also developed.

- The proposed models apply to both APT and SPT schemes. In that sense, it can be considered as a generalization of the analytical models proposed for the SPT scheme like [7], [12]. Note also that in the studied APT scheme the size of a frame may change randomly from cycle to cycle, as described with more detail in Algorithm 1 of the next section.
- Closed-form expressions for calculating mean packet delay, throughput, packet loss probability, energy consumption, and energy efficiency are obtained based on the proposed models. Furthermore, the analytical model has been shown to be very accurate, when compared with discrete-event based simulations.

III. NETWORK MODEL

In this section, we give a brief description of the operation of S-MAC, introduce the network scenario and the assumptions of the study, and provide expressions that model the access to the medium of nodes in a WSN operated on S-MAC.

A. Brief Description of S-MAC

In S-MAC the time is partitioned into cycles of equal length T , and each cycle contains an *active* and a *sleep* period. The *active* period is further divided into two parts: the *sync* period of fixed length T_{sync} , where SYNC packets are exchanged, and the *data* period, where DATA packets are exchanged. Throughout this paper, we use capital letters to represent the type of a packet. For example, DATA, SYNC and RTS are the packets. Conversely, we use lowercase letters to represent the different parts of a cycle: *active*, *sleep*, *sync* and *data*.

In a *sync* period, every node chooses a sleep-awake schedule and exchanges it with its neighbors using SYNC packets. These packets include the address of the sender and the time of its next *active* period initiation. With this information, nodes are able to coordinate to wake up at the same time at the beginning of the next cycle. In the considered network, all nodes are awake at the start of a *sync* period and might broadcast a SYNC packet. To this end they follow a CSMA/CA mechanism for contention-based channel access. It is based on generating a random backoff time and performing a carrier sensing procedure. If the channel is idle when the backoff timer expires, then the node transmits the SYNC packet.

Refer to a set of N_{sc} consecutive cycles as an *update* super-cycle. As in [7], we assume for simplicity that nodes transmit one SYNC packet every N_{sc} cycles, i.e., one packet per *update* super-cycle, and it might receive one SYNC packet per cycle in the remaining $N_{sc} - 1$ cycles.

In order to avoid missing SYNC packets from neighboring nodes, from now and then a node keeps awake for the whole cycle. As these cycles are different from the *normal* cycles which include both *active* and *sleep* periods, we refer to them

as *awake* cycles. Define a hyper-cycle as a set of N_{aw} *update* super-cycles, i.e., $N_{aw} \cdot N_{sc}$ consecutive cycles. We assume that a node follows *awake* cycles during a complete super-cycle (N_{sc} consecutive cycles), while it follows *normal* cycles during the other $N_{aw} - 1$ *update* super-cycles of the hyper-cycle. The characteristics of *normal* and *awake* cycles will be later used to determine the average energy consumed by a node.

Nodes might transmit a *DATA* packet during the *data* period using a CSMA/CA mechanism for contention-based channel access. To this end, they generate new backoff times at each *data* period initiation and perform carrier sense. If the channel is idle when the backoff timer expires, then the node can transmit the *DATA* packet using an RTS/CTS/*DATA*/ACK handshake. When a winning node receives *CTS* in response to its previous *RTS*, it transmits one *DATA* frame. In S-MAC, a node goes to *sleep* until the beginning of next *sync* period when: i) it loses the contention (hears a busy medium before its backoff time expires); ii) it encounters an *RTS* collision or *CTS* is lost; and iii) after the reception of an *ACK* as a response to a successful frame transmission. Recall that each *sync* period is followed by a *data* (*listen*) period. For further details on S-MAC please refer to [1].

B. Network Scenario and Assumptions

Consider a cluster of N sensor nodes that transmit packets towards a single destination node, i.e., the *sink*, as shown in Figure 1. For convenience, we select one of the N nodes arbitrarily, and refer to it as the reference node (RN). We assume that the sink node behaves as a packet absorption node, i.e., it only receives packets (it never transmits). All nodes are one hop away from each other forming a *single-cell* cluster, but multiple clusters together may form a larger network.

A node is capable of buffering a finite number, Q , of packets, and it serves them according to a first in first out (FIFO) discipline. A node performs packet aggregation based on the number of packets accumulated in its queue. A set of packets aggregated according to the following rule will be referred to as a *frame*. The transmission of a frame by the RN happens when it wins the contention for medium access. If the number of packets in its queue is smaller than the maximum allowed frame size F , then a frame containing all the packets in the queue is transmitted. However, if the number of packets in its queue is greater than or equal to F , then a frame containing F packets is transmitted. If the transmission is successful, then the number of packets in the queue of the RN is decremented by the frame size.

For clarity, the packet aggregation scheme is described in Algorithm 1. Note that the APT scheme presented here is not a MAC protocol itself, but it is a possible mode for the operation of S-MAC. That is, to obtain channel access, the RN has to contend with other nodes according to S-MAC as explained before. Observe that the proposed APT scheme is general and it is applicable to any synchronous DC MAC protocol as well.

The operation of S-MAC with APT is illustrated in Figure 2. In the figure, the RN wins the contention in the cycle and a frame is sent to the sink node. As in conventional SPT S-MAC

scenarios, all other active nodes go to sleep after receiving *RTS* from the RN. Therefore, for these nodes the *data* period lasts merely until the reception of *RTS*. However, the duration of the *data* period for the RN depends on the transmitted frame size. Observe that the duration of the *data* period is constrained by the length of the cycle and therefore, it must be shorter than or equal to $T - T_{sync}$. This provides an upper bound for the maximum allowed frame size F . A node drops a frame when the number of consecutive retransmissions of the same frame reaches the maximum number of allowed retransmissions, R .

Note also that, as the buffer has finite capacity, packet loss due to buffer overflow might happen when packets arrive and find a full buffer. During overflow episodes, some degree of selective packet discarding must occur at the nodes to give priority to the most important information. Once such imperative information is selected, nodes will deploy retransmissions in order to achieve a loss free transfer across the network.

In this study, we assume that: i) all nodes contain the same initial energy; ii) the channel is error-free (for 2D and 3D models), or error-prone (for 4D model); iii) transmission failure happens either only due to collision in the medium (for 2D and 3D models) or due to both collision and channel failure (for 4D model); iv) packets arrive to the buffer of a node following a renewal arrival process, and the number of packets that arrive per cycle is characterized by independent and identically distributed random variables. For simplicity, we assume that the number of packets that arrive to a buffer follow a discrete Poisson distribution of mean λT , where λ is the packet arrival rate and T is the cycle duration.

C. Access to the Medium

According to the operation of S-MAC, at each cycle, nodes with a non-empty queue generate a random backoff time taken from $\{0, W - 1\}$. When the RN is active, it transmits a frame successfully when the other contending nodes select backoff times longer than the one selected by the RN. A frame transmitted by the RN will fail (collide) when the RN and one or more of the other contending nodes select the same backoff time, and this backoff time is the smallest among all contending nodes. If the backoff time generated by the RN is not the smallest one among those generated by the

Algorithm 1: Aggregated Packet Transmission by the RN

```

1 begin
2   input:
3      $i$  = Number of packets in the queue of a node
4      $F$  = Maximum size of a frame
5   output:
6      $f$  = Number of packets aggregated in the frame
7      $q$  = Number of packets left in the queue after frame transmission
8   if the RN wins medium access then
9     if  $i \leq F$  then
10      | transmit  $i$  packets in the frame,  $f = i$ ,  $q = 0$ ;
11     end
12     else if  $i > F$  then
13      | transmit  $F$  packets,  $f = F$ ,  $q = i - F$ ;
14     end
15   end
16 end
```

The transition probabilities of this DTMC are defined in Table II. Note that when the transition between two states is not possible, its transition probability is zero. For brevity, zero transition probabilities are not shown in the table. As an example, we explain $P_{(i,k,0),(j,l,0)}$, i.e., the transition probability from State $(i, k, 0)$ to State $(j, l, 0)$. It is given by,

$$\begin{aligned} P_{(i,k,0),(j,l,0)} = & P_{s,k} \cdot B_{l-k}(K-k) \cdot A_{j-i+\alpha} \\ & + kP_{s,k} \cdot P_e \cdot B_{l-k+1}(K-k) \cdot A_{j-i} \\ & + kP_{s,k} \cdot \hat{P}_e \cdot B_{l-k}(K-k) \cdot A_{j-i} \\ & + \hat{T}_k \cdot B_{l-k}(K-k) \cdot A_{j-i}. \end{aligned}$$

$i - \alpha \leq j < Q, 0 \leq l - k \leq l, l < K.$

The first term defines the probability that the RN wins the contention, it transmits a frame composed of $\alpha = \min(i, F)$ packets, it receives $j - i + \alpha$ packets and $l - k$ nodes out of the $K - k$ inactive ones become active. The second term defines the probability that an active node different from the RN wins the contention, it transmits a frame successfully and its buffer becomes empty (P_e), and therefore the node becomes inactive, $l - k + 1$ nodes out of the $K - k$ inactive ones become active, and the RN receives $j - i$ packets. The third term defines the probability that an active node different from the RN wins the contention, it transmits a frame successfully but its buffer does not become empty (\hat{P}_e), $l - k$ nodes out of the $K - k$ inactive ones become active, and the RN receives $j - i$ packets. Lastly, the fourth term defines the probability that the RN does not transmit when contending with other k nodes and two or more of the other nodes collide (\hat{T}_k), $l - k$ nodes out of the $K - k$ inactive ones become active, and the RN receives $j - i$ packets. Note that in the last term it is assumed that, for any of the nodes that collide, the probability that it discards a frame and becomes inactive is negligible.

The solution of this aperiodic and irreducible DTMC is obtained by solving the set of linear equations

$$\pi \mathbf{P} = \pi, \quad \pi \mathbf{e} = \mathbf{1}, \quad (3)$$

where π is the stationary distribution, \mathbf{P} is the transition probability matrix, whose elements are defined in Table II, and \mathbf{e} is a column vector of ones. The elements of the distribution π are $\pi(i, k, r)$, i.e., the fraction of cycles where the RN is in State (i, k, r) . To determine

$$P_e = \frac{P_s A_0 \sum_{i=1}^F \pi_i}{P_s (1 - \pi_0)}, \quad (4)$$

the stationary distribution π is required, where P_s is the average probability that an active node transmits a frame successfully in a random cycle conditioned on being active, and π_i is the stationary probability of finding i packets in the queue of a node. Note that P_e is a conditional probability. Its denominator is the fraction of cycles where the RN transmits a frame successfully. While its numerator is the fraction of cycles where the RN successfully transmits a frame that empties the buffer and no additional packets arrive. P_s and

π_i can be determined by

$$P_s = \frac{1}{G} \sum_{i=1}^Q \sum_{k=0}^K \sum_{r=0}^R \pi(i, k, r) \cdot P_{s,k}, \quad (5)$$

$$\pi_i = \sum_{k=0}^K \sum_{r=0}^R \pi(i, k, r), \quad (6)$$

where $G = \sum_{i=1}^Q \sum_{k=0}^K \sum_{r=0}^R \pi(i, k, r)$.

By solving the set of equations (3), $\pi(P_s)$ can be determined for a given P_s . Then, a new $P_s(\pi)$ can be obtained from (5) for a given π . Denote by P_s the solution of this fixed-point equation, i.e., the value of $P_s(\pi)$ at the fixed-point. Note that the stationary distribution for the 3D DTMC that defines the operation of the SPT scheme with finite retransmissions can be readily obtained by setting $F = 1$.

Note that finding a good estimation for the distribution of the number of active nodes in a cycle is crucial to determine with precision P_s , the stationary distribution π , and the performance parameters defined later in Section V. In [12] we compared the accuracy of different performance parameters obtained when two different approaches are used to characterize the number of active nodes in a cycle. That is, i) when it is assumed that nodes become active independently, as done for example in [7], [11], and the number of active nodes in a cycle follows a binomial distribution; and ii) when the number of active nodes in the network is represented in the network state vector and evolves from cycle to cycle, as done in the model proposed here. The study concludes that substantially more accurate results are obtained when the second approach is adopted.

B. 2D DTMC for APT with Infinite Retransmissions

The main objective of the proposed 3D DTMC model is to evaluate the performance of a WSN that employs an APT scheme on a synchronous DC MAC when frame retransmissions are enabled. As it will be shown later in Section VI, a vast majority of the frames require at most two retransmissions to achieve a successful transmission. Therefore, the same performance would be observed by setting $R \geq 2$. This observation motivated us to develop a simpler 2D DTMC model to evaluate the performance of APT with infinite retransmissions.

We adopt the same notation used for the 3D DTMC, except that the dimension related to the number of retransmissions, r , is omitted. A state in the 2D DTMC is represented by (i, k) , where i is the number of packets in the queue of the RN, $i \leq Q$, and k is the number of active nodes other than the RN in the network, $k \leq K = N - 1$. Then, $P_{(i,k),(j,l)}$ is the transition probability from State (i, k) to State (j, l) .

The transition probabilities of the proposed 2D DTMC are given in Table III. In the table, the first row defines transitions caused only by new arrivals when the RN has an empty queue and no other node is active. The second row describes transmissions made by the other nodes while the RN has an empty queue. The third and fourth rows define RN's transmissions in cycles where there is no other active node and when there are other active nodes respectively. Lastly, the fifth row defines transitions that are not possible.

TABLE II
TRANSITION PROBABILITIES OF THE 3D DTMC MODEL FOR S-MAC-APT WITH FINITE RETRANSMISSIONS

No active node exists. Transitions occur due to new arrivals	
$P_{(0,0,0),(j,l,0)} = B_l(K) \cdot A_j; 0 \leq j < Q, 0 \leq l \leq K,$	$P_{(0,0,0),(Q,l,0)} = B_l(K) \cdot A_{\geq Q}; 0 \leq l \leq K.$
No packets in the queue of the RN, i.e., no transmissions by the RN. Transitions are caused by the other k active nodes	
$P_{(0,k,0),(j,l,0)} = S_k \cdot P_e \cdot B_{l-k+1}(K-k) \cdot A_j$ $+ S_k \cdot \hat{P}_e \cdot B_{l-k}(K-k) \cdot A_j$ $+ \hat{S}_k \cdot B_{l-k}(K-k) \cdot A_j;$ $0 \leq j < Q, 1 \leq k \leq l < K,$	$P_{(0,k,0),(Q,l,0)} = S_k \cdot P_e \cdot B_{l-k+1}(K-k) \cdot A_{\geq Q}$ $+ S_k \cdot \hat{P}_e \cdot B_{l-k}(K-k) \cdot A_{\geq Q}$ $+ \hat{S}_k \cdot B_{l-k}(K-k) \cdot A_{\geq Q};$ $1 \leq k \leq l < K,$
$P_{(0,k,0),(j,K,0)} = S_k \cdot \hat{P}_e \cdot B_{K-k}(K-k) \cdot A_j$ $+ \hat{S}_k \cdot B_{K-k}(K-k) \cdot A_j;$ $0 \leq j < Q, 1 \leq k \leq K,$	$P_{(0,k,0),(Q,K,0)} = S_k \cdot \hat{P}_e \cdot B_{K-k}(K-k) \cdot A_{\geq Q}$ $+ \hat{S}_k \cdot B_{K-k}(K-k) \cdot A_{\geq Q};$ $1 \leq k \leq K,$
$P_{(0,k,0),(j,k-1,0)} = S_k \cdot P_e \cdot B_0(K-k) \cdot A_j;$ $0 \leq j < Q, 1 \leq k \leq K,$	$P_{(0,k,0),(Q,k-1,0)} = S_k \cdot P_e \cdot B_0(K-k) \cdot A_{\geq Q};$ $1 \leq k \leq K.$
$k+1$ nodes including the RN are active. Successful transmission by the RN in its first attempt or by any other node	
$P_{(i,k,0),(j,l,0)} = P_{s,k} \cdot B_{l-k}(K-k) \cdot A_j$ $1 \leq i \leq F, 0 \leq j \leq i-1, 0 \leq k \leq l \leq K,$	$P_{(i,k,0),(j,l,0)} = P_{s,k} \cdot B_{l-k}(K-k) \cdot A_{j-i+F}$ $F+1 \leq i \leq Q, i-F \leq j \leq i-1, 0 \leq k \leq l \leq K,$
$P_{(i,k,0),(j,l,0)} = P_{s,k} \cdot B_{l-k}(K-k) \cdot A_{j-i+\alpha}$ $+ kP_{s,k} \cdot P_e \cdot B_{l-k+1}(K-k) \cdot A_{j-i}$ $+ kP_{s,k} \cdot \hat{P}_e \cdot B_{l-k}(K-k) \cdot A_{j-i}$ $+ \hat{T}_k \cdot B_{l-k}(K-k) \cdot A_{j-i};$ $1 \leq i \leq j < Q, 1 \leq k \leq l < K,$	$P_{(i,k,0),(Q,l,0)} = P_{s,k} \cdot B_{l-k}(K-k) \cdot A_{\geq Q-i+\alpha}$ $+ kP_{s,k} \cdot P_e \cdot B_{l-k+1}(K-k) \cdot A_{\geq Q-i}$ $+ kP_{s,k} \cdot \hat{P}_e \cdot B_{l-k}(K-k) \cdot A_{\geq Q-i}$ $+ \hat{T}_k \cdot B_{l-k}(K-k) \cdot A_{\geq Q-i};$ $1 \leq i \leq Q, 1 \leq k \leq l < K,$
$P_{(i,k,0),(j,K,0)} = P_{s,k} \cdot B_{K-k}(K-k) \cdot A_{j-i+\alpha}$ $+ kP_{s,k} \cdot \hat{P}_e \cdot B_{K-k}(K-k) \cdot A_{j-i};$ $+ \hat{T}_k \cdot B_{l-k}(K-k) \cdot A_{j-i};$ $1 \leq i \leq j < Q, 1 \leq k \leq K,$	$P_{(i,k,0),(Q,K,0)} = P_{s,k} \cdot B_{K-k}(K-k) \cdot A_{\geq Q-i+\alpha}$ $+ kP_{s,k} \cdot \hat{P}_e \cdot B_{K-k}(K-k) \cdot A_{\geq Q-i};$ $+ \hat{T}_k \cdot B_{l-k}(K-k) \cdot A_{\geq Q-i};$ $1 \leq i \leq Q, 1 \leq k \leq K.$
$k+1$ nodes including the RN are active. Successful transmission by the RN after r failed attempts	
$P_{(i,k,r),(j,l,0)} = P_{s,k} \cdot B_{l-k}(K-k) \cdot A_j$ $1 \leq i \leq F, 0 \leq j \leq i-1, 0 \leq k \leq l < K,$ $0 \leq r \leq R,$	$P_{(i,k,r),(j,l,0)} = P_{s,k} \cdot B_{l-k}(K-k) \cdot A_{j-i+F}$ $F+1 \leq i \leq Q, i-F \leq j \leq i-1, 0 \leq k \leq l \leq K,$ $0 \leq r \leq R,$
$P_{(i,k,r),(j,l,0)} = P_{s,k} \cdot B_{l-k}(K-k) \cdot A_{j-i+\alpha}$ $1 \leq i \leq j < Q, 0 \leq k \leq l \leq K, 0 \leq r \leq R,$	$P_{(i,k,r),(Q,l,0)} = P_{s,k} \cdot B_{l-k}(K-k) \cdot A_{\geq Q-i+\alpha}$ $1 \leq i \leq Q, 0 \leq k \leq l \leq K, 0 \leq r \leq R,$
$k+1$ nodes including the RN are active. Failed transmission by the RN	
$P_{(i,k,r),(j,l,r+1)} = P_{f,k} \cdot B_{l-k}(K-k) \cdot A_{j-i}$ $1 \leq i \leq j < Q, 0 \leq k \leq l \leq K, 0 \leq r < R,$	$P_{(i,k,r),(Q,l,r+1)} = P_{f,k} \cdot B_{l-k}(K-k) \cdot A_{\geq Q-i}$ $1 \leq i \leq Q, 0 \leq k \leq l \leq K, 0 \leq r < R.$
$P_{(i,k,R),(j,l,0)} = P_{f,k} \cdot B_{l-k}(K-k) \cdot A_{j-i+\alpha}$ $1 \leq i \leq Q, i-\alpha \leq j < Q, 0 \leq k \leq l \leq K,$	$P_{(i,k,R),(Q,l,r+1)} = P_{f,k} \cdot B_{l-k}(K-k) \cdot A_{\geq Q-i+\alpha}$ $1 \leq i \leq Q, 0 \leq k \leq l \leq K.$
$k+1$ nodes including the RN are active. The RN loses access contention	
$P_{(i,k,r),(j,l,r)} = kP_{s,k} \cdot P_e \cdot B_{l-k+1}(K-k) \cdot A_{j-i}$ $+ kP_{s,k} \cdot \hat{P}_e \cdot B_{l-k}(K-k) \cdot A_{j-i}$ $+ \hat{T}_k \cdot B_{l-k}(K-k) \cdot A_{j-i};$ $1 \leq i \leq j < Q, 1 \leq k < K, 0 \leq r \leq R,$	$P_{(i,k,r),(Q,l,r)} = kP_{s,k} \cdot P_e \cdot B_{l-k+1}(K-k) \cdot A_{\geq Q-i}$ $+ kP_{s,k} \cdot \hat{P}_e \cdot B_{l-k}(K-k) \cdot A_{\geq Q-i}$ $+ \hat{T}_k \cdot B_{l-k}(K-k) \cdot A_{\geq Q-i};$ $1 \leq i \leq Q, 1 \leq k < K, 0 \leq r \leq R,$
$P_{(i,K,r),(j,K,r)} = kP_{s,k} \cdot \hat{P}_e \cdot B_{K-k}(K-k) \cdot A_{j-i}$ $+ \hat{T}_k \cdot B_{K-k}(K-k) \cdot A_{j-i};$ $1 \leq i \leq j < Q, 0 \leq r \leq R,$	$P_{(i,K,r),(Q,K,r)} = kP_{s,k} \cdot \hat{P}_e \cdot B_{K-k}(K-k) \cdot A_{\geq Q-i}$ $+ \hat{T}_k \cdot B_{K-k}(K-k) \cdot A_{\geq Q-i};$ $1 \leq i \leq Q, 0 \leq r \leq R,$
$P_{(i,k,r),(j,k-1,r)} = kP_{s,k} \cdot P_e \cdot B_0(K-k) \cdot A_{j-i};$ $1 \leq i \leq j < Q, 1 \leq k \leq K, 0 \leq r \leq R,$	$P_{(i,k,r),(Q,k-1,r)} = kP_{s,k} \cdot P_e \cdot B_0(K-k) \cdot A_{\geq Q-i};$ $1 \leq i \leq Q, 1 \leq k \leq K, 0 \leq r \leq R.$

The stationary distribution can be determined by solving the set of linear equations (3), where the transition probability matrix \mathbf{P} is now defined in Table III. As in the 3D DTMC, P_s is found as the solution of a fixed-point equation where

$$P_s = \frac{1}{G} \sum_{i=1}^Q \sum_{k=0}^K \pi(i, k) \cdot P_{s,k}, \quad (7)$$

$$\pi_i = \sum_{k=0}^K \pi(i, k), \quad (8)$$

and $G = \sum_{i=1}^Q \sum_{k=0}^K \pi(i, k)$. Similarly, the stationary distri-

bution for the 2D DTMC that defines the operation of the SPT scheme with infinite retransmissions can be readily obtained by configuring $F = 1$.

V. PERFORMANCE PARAMETERS

In this section, we derive expressions for average packet delay, throughput, packet loss probability, average energy consumption per cycle, and energy efficiency for S-MAC operating on both the APT and the SPT schemes. Recall that the 2D and 3D models are developed based on the assumption that the channel is error-free.

TABLE III
TRANSITION PROBABILITIES OF THE 2D DTMC MODEL FOR S-MAC-APT WITH INFINITE RETRANSMISSIONS

No active node exists. Transitions occur due to new arrivals	
$P_{(0,0),(j,l)} = B_l(K) \cdot A_j; 0 \leq j < Q, 0 \leq l \leq K,$	$P_{(0,0),(Q,l)} = B_l(K) \cdot A_{\geq Q}; 0 \leq l \leq K.$
No packets in the queue of the RN, i.e., no transmissions by the RN. Transitions are caused by the other k active nodes	
$P_{(0,k),(j,l)} = S_k \cdot P_e \cdot B_{l-k+1}(K-k) \cdot A_j$ $+ S_k \cdot \hat{P}_e \cdot B_{l-k}(K-k) \cdot A_j$ $+ \hat{S}_k \cdot B_{l-k}(K-k) \cdot A_j;$ $0 \leq j < Q, 1 \leq k \leq l < K,$	$P_{(0,k),(Q,l)} = S_k \cdot P_e \cdot B_{l-k+1}(K-k) \cdot A_{\geq Q}$ $+ S_k \cdot \hat{P}_e \cdot B_{l-k}(K-k) \cdot A_{\geq Q}$ $+ \hat{S}_k \cdot B_{l-k}(K-k) \cdot A_{\geq Q};$ $1 \leq k \leq l < K,$
$P_{(0,k),(j,K)} = S_k \cdot \hat{P}_e \cdot B_{K-k}(K-k) \cdot A_j,$ $+ \hat{S}_k \cdot B_{K-k}(K-k) \cdot A_j;$ $0 \leq j < Q, 1 \leq k \leq K,$	$P_{(0,k),(Q,K)} = S_k \cdot \hat{P}_e \cdot B_{K-k}(K-k) \cdot A_{\geq Q},$ $+ \hat{S}_k \cdot B_{K-k}(K-k) \cdot A_{\geq Q};$ $1 \leq k \leq K.$
$P_{(0,k),(0,k-1)} = S_k \cdot P_e \cdot B_0(K-k) \cdot A_j;$ $0 \leq j < Q, 1 \leq k \leq K,$	$P_{(0,k),(Q,k-1)} = S_k \cdot P_e \cdot B_0(K-k) \cdot A_{\geq Q};$ $1 \leq k \leq K,$
The RN is the only active node	
$P_{(i,0),(j,l)} = P_{s,0} \cdot B_l(K) \cdot A_j$ $1 \leq i \leq F, 0 \leq j \leq i-1, 0 \leq l \leq K,$	$P_{(i,0),(j,l)} = P_{s,0} \cdot B_l(K) \cdot A_{j-i+F}$ $F+1 \leq i \leq Q, i-F \leq j \leq i-1, 0 \leq l \leq K,$
$P_{(i,0),(j,l)} = P_{s,0} \cdot B_l(K) \cdot A_{j-i+\alpha}$ $1 \leq i \leq j < Q, 0 \leq l \leq K,$	$P_{(i,0),(Q,l)} = P_{s,0} \cdot B_l(K) \cdot A_{\geq Q-i+\alpha}$ $1 \leq i \leq Q, 0 \leq k \leq K.$
Contention: transitions are caused by $k+1$ active nodes including the RN	
$P_{(i,k),(j,l)} = P_{s,k} \cdot B_{l-k}(K-k) \cdot A_j$ $1 \leq i \leq F, 0 \leq j \leq i-1, 0 \leq k \leq l < K,$	$P_{(i,k),(j,l)} = P_{s,k} \cdot B_{l-k}(K-k) \cdot A_{j-i+F}$ $F+1 \leq i \leq Q, i-F \leq j \leq i-1, 0 \leq k \leq l \leq K,$
$P_{(i,k),(j,l)} = P_{s,k} \cdot B_{l-k}(K-k) \cdot A_{j-i+\alpha}$ $+ k P_{s,k} \cdot P_e \cdot B_{l-k+1}(K-k) \cdot A_{j-i}$ $+ k P_{s,k} \cdot \hat{P}_e \cdot B_{l-k}(K-k) \cdot A_{j-i}$ $+ \hat{S}_{k+1} \cdot B_{l-k}(K-k) \cdot A_{j-i};$ $1 \leq i \leq j < Q, 1 \leq k \leq l < K,$	$P_{(i,k),(Q,l)} = P_{s,k} \cdot B_{l-k}(K-k) \cdot A_{\geq Q-i+\alpha}$ $+ k P_{s,k} \cdot P_e \cdot B_{l-k+1}(K-k) \cdot A_{\geq Q-i}$ $+ k P_{s,k} \cdot \hat{P}_e \cdot B_{l-k}(K-k) \cdot A_{\geq Q-i}$ $+ \hat{S}_{k+1} \cdot B_{l-k}(K-k) \cdot A_{\geq Q-i};$ $1 \leq i \leq Q, 1 \leq k \leq l < K,$
$P_{(i,k),(j,K)} = P_{s,k} \cdot B_{K-k}(K-k) \cdot A_{j-i+\alpha}$ $+ k P_{s,k} \cdot \hat{P}_e \cdot B_{K-k}(K-k) \cdot A_{j-i}$ $+ \hat{S}_{k+1} \cdot B_{K-k}(K-k) \cdot A_{j-i};$ $1 \leq i \leq j < Q, 1 \leq k \leq K,$	$P_{(i,k),(Q,K)} = P_{s,k} \cdot B_{K-k}(K-k) \cdot A_{\geq Q-i+\alpha}$ $+ k P_{s,k} \cdot \hat{P}_e \cdot B_{K-k}(K-k) \cdot A_{\geq Q-i}$ $+ \hat{S}_{k+1} \cdot B_{K-k}(K-k) \cdot A_{\geq Q-i};$ $1 \leq i \leq Q, 1 \leq k \leq K,$
$P_{(i,k),(j,k-1)} = k P_{s,k} \cdot P_e \cdot B_0(K-k) \cdot A_{j-i}$ $1 \leq i \leq j < Q, 1 \leq k \leq K,$	$P_{(i,k),(Q,k-1)} = k P_{s,k} \cdot P_e \cdot B_0(K-k) \cdot A_{\geq Q-i}$ $1 \leq i \leq Q, 1 \leq k \leq K.$
Impossible transitions	
$P_{(i,k),(j,k-1)} = 0; 1 \leq i \leq Q, j < i, 1 \leq k \leq K,$	$P_{(i,k),(j,l)} = 0; F+1 \leq i \leq Q, j < i-F,$
$P_{(i,k),(j,l)} = 0, 0 \leq i \leq j \leq Q, 2 \leq k \leq K, l \leq k-2,$	$0 \leq k \leq l \leq K.$

A. Average Packet Delay

Let D be the average delay that a packet experiences from its arrival until it is successfully transmitted. Then, D can be determined by applying Little's law,

$$D = \frac{N_{av}}{\gamma_a}, \quad N_{av} = \sum_{i=0}^Q i \pi_i, \quad \gamma_a = \sum_{i=0}^Q b_i \pi_i, \quad (9)$$

where $b_0 = \sum_{q=0}^Q q \cdot A_q + Q \cdot A_{\geq Q+1}$ and $b_i = \sum_{q=0}^{Q-i} q \cdot A_q + (Q-i+P_s) A_{\geq Q-i+1}$, $i > 0$. Note that: i) π_i is the stationary probability of finding i packets in the queue of the RN, and is determined by expressions (6) or (8); ii) N_{av} is the average number of packets in the queue; iii) γ_a is the average number of packets that entered the queue (*accepted*) per cycle; and iv) b_i is the mean number of packets *accepted* per cycle at state i . Note also that the last term of b_i is obtained from $((Q-i+1)P_s + (Q-i)(1-P_s))A_{\geq Q-i+1}$.

B. Throughput

We define the node throughput, η , as the average number of packets successfully delivered by a node in a cycle. For

the 3D and 2D DTMCs, η can be determined respectively as follows.

$$\eta = \begin{cases} \sum_{i=1}^Q \sum_{k=0}^K \sum_{r=0}^R \alpha \cdot \pi(i, k, r) \cdot P_{s,k} & \text{for 3D} \\ \sum_{i=1}^Q \sum_{k=0}^K \alpha \cdot \pi(i, k) \cdot P_{s,k} & \text{for 2D} \end{cases} \quad (10)$$

Recall that $\alpha = \min(i, F)$. In a network composed of N sensor nodes, the *total network throughput* expressed in packets per cycle is given by

$$Th = N \cdot \eta. \quad (11)$$

C. Packet Loss Probability

Since the channel is assumed to be error-free, two causes might lead to a packet drop: i) it encounters the buffer full upon arrival; i.e., it might be discarded due to buffer overflow; ii) its transmission fails after R retransmissions. Recall that R is the maximum number of retransmissions allowed for a frame. The average number of packets lost per cycle due to buffer overflow is $\lambda T - \gamma_a$, where λT is the mean number of packets that arrived per cycle, and γ_a is the average number of packets accepted in the queue per cycle (9).

For the 3D DTMC that models a system with finite retransmissions, let P_L^c denote the packet loss probability due to collisions,

$$P_L^c = \frac{1}{H} \sum_{i=1}^Q \sum_{k=0}^K \alpha \cdot \pi(i, k, R) \cdot P_{f,k}, \quad (12)$$

where $H = \sum_{i=1}^Q \sum_{k=0}^K \sum_{r=0}^{R-1} \alpha \cdot \pi(i, k, r) \cdot P_{s,k} + \sum_{i=1}^Q \sum_{k=0}^K \alpha \cdot \pi(i, k, R) \cdot P_{sf,k}$. Note that once the packet is in the queue, it will be either successfully transmitted or dropped. Then, P_L^c is the fraction of accepted packets that are discarded after R consecutive unsuccessful retransmissions. Since H is the average number of packets transmitted per cycle successfully or with failure, it must be equal to the average number of packets accepted at the queue per cycle γ_a .

The total packet loss probability, including buffer overflow and packet losses due to collisions in the medium, can be determined by,

$$P_L = 1 - \frac{(1 - P_L^c) \gamma_a}{\lambda T}. \quad (13)$$

Note that in the 2D case, packet loss is only due to buffer overflow since a packet which encounters collisions will be retransmitted until it is successfully received.

D. Average Energy Consumption

As described in Section III, the *active* period of a cycle is further divided into the *sync* and *data* periods. The energy consumed during the *active* period represents the dominant contribution to the total energy consumption. In this subsection we calculate the energy consumed by the RN in the *sync*, *data* and *sleep* periods. Note that we only study the energy consumed by the radio frequency transceiver. The energy consumed by the sensor nodes due to their event sensing tasks is application dependent and is not included here.

1) *Energy Consumption in the sync Period:* Denote by $T_{sync} = (W - 1) + t_{SYNC} + D_p$ the duration of a *sync* period. Recall that we assume for simplicity that the RN *broadcasts* one *SYNC* packet every N_{sc} cycles, i.e., one packet per *update* super-cycle, and receives one packet per cycle in the remaining $N_{sc} - 1$ cycles. Accordingly, the energy consumed by the RN in the *sync* period is given by,

$$E_{sc} = \frac{1}{N_{sc}} \cdot [(t_{SYNC} \cdot P_{tx} + (T_{sync} - t_{SYNC}) \cdot P_{rx})] + \frac{N_{sc} - 1}{N_{sc}} \cdot (T_{sync} \cdot P_{rx}), \quad (14)$$

where P_{tx} and P_{rx} are the transmission and reception power levels respectively. Note that in the transmission of the *SYNC* packet, the RN consumes energy for carrier sensing as well, and this energy consumption is already included in the second part of the first term in (14).

2) *Energy Consumption in the data Period:* In the APT scheme, the number of packets aggregated in a frame depends on the number of packets available in the queue at the transmission time. The average size of a frame transmitted

by the RN when it contends with other k nodes, f_k , can be obtained by

$$f_k = \begin{cases} \frac{1}{G_k} \sum_{i=1}^Q \sum_{r=0}^R \alpha \cdot \pi(i, k, r) & \text{for 3D} \\ \frac{1}{G_k} \sum_{i=1}^Q \alpha \cdot \pi(i, k) & \text{for 2D} \end{cases} \quad (15)$$

where $\alpha = \min(i, F)$, $G_k = \sum_{i=1}^Q \sum_{r=0}^R \pi(i, k, r)$ for the 3D DTMC, and $G_k = \sum_{i=1}^Q \pi(i, k)$ for the 2D DTMC, $0 \leq k \leq N - 1$, respectively. Note that $f_k = 1$ for the SPT scheme.

In order to calculate the average energy consumed in the *data* period of a cycle, we consider the following constants associated with the RN during: i) a successful transmission when it contends with other k nodes $E_{txs,k} = (t_{RTS} + f_k \cdot t_{DATA}) \cdot P_{tx} + (t_{CTS} + t_{ACK}) \cdot P_{rx}$, ii) a transmission failure (collision) $E_{txf} = t_{RTS} \cdot P_{tx} + t_{CTS} \cdot P_{rx}$, and iii) during overhearing situations $E_{oh} = E_{oh} = t_{RTS} \cdot P_{rx}$, where t_{RTS} , t_{DATA} , t_{CTS} and t_{ACK} are the corresponding packet transmission times. Recall that nodes address their frames to the sink, and that the sink receives but does not transmit. Then, the average energy consumed by the RN during the *data* period of a cycle when it contends with other k nodes, $k \geq 1$, is obtained by

$$E_{d,k+1} = q_{1,k} P_{s,k} \cdot [E_{txs,k} + (4D_p + BT_{s,k}) \cdot P_{rx}] + q_{1,k} P_{f,k} \cdot [E_{txf} + (2D_p + BT_{f,k}) \cdot P_{rx}] + q_{2,k} P_{s,k} [E_{oh} + (D_p + BT_{s,k}) \cdot P_{rx}] + q_{3,k} \cdot [E_{oh} + (D_p + BT_{f,k}) \cdot P_{rx}], \quad (16)$$

where D_p is the one-way propagation delay. Conditioned on finding $k+1$ nodes active, $q_{1,k} = (k+1)/N$ is the probability that the RN is active, $q_{2,k} = kq_{1,k} + (k+1)(1 - q_{1,k})$ is the average number of active nodes other than the RN, and $q_{3,k} = 1 - q_{2,k}P_{s,k} - q_{1,k}P_{sf,k}$ is the probability that nodes other than the RN transmit a frame with failure. Note that the terms in $E_{d,k+1}$ correspond to the energy consumed by: a frame successfully transmitted, a frame transmitted that collides, overhearing a successful frame transmitted by nodes other than the RN, and overhearing a collision of frames transmitted by nodes other than the RN, respectively. Also, $E_{d,1} = q_{1,0} \cdot [E_{txs,0} + (4D_p + (W - 1)/2) \cdot P_{rx}] + q_{2,0} \cdot [E_{oh} + (D_p + (W - 1)/2) \cdot P_{rx}]$, and $E_{d,0} = (t_{RTS} + W + D_p) \cdot P_{rx}$.

3) *Energy Consumption in the sleep Period:* When $k+1$ active nodes contend in a cycle, where $k \geq 1$, the average energy consumed by the RN during the *sleep* period of an *awake* cycle is given by,

$$E_{aw,k+1} = q_{1,k} P_{s,k} \cdot [(T - T_{sync} - T_{d,s,k}) \cdot P_{rx}] + q_{1,k} P_{f,k} \cdot [(T - T_{sync} - T_{d,f,k}) \cdot P_{rx}] + q_{2,k} P_{s,k} [(T - T_{sync} - T_{d,os,k}) \cdot P_{rx}] + q_{3,k} \cdot [(T - T_{sync} - T_{d,of,k}) \cdot P_{rx}], \quad (17)$$

where $T_{d,s,k} = t_{RTS} + f_k \cdot t_{DATA} + t_{CTS} + t_{ACK} + 4D_p + BT_{s,k}$, $T_{d,f,k} = t_{RTS} + t_{CTS} + 2D_p + BT_{f,k}$, $T_{d,os,k} = t_{RTS} + D_p + BT_{s,k}$, and $T_{d,of,k} = t_{RTS} + D_p + BT_{f,k}$. These terms represent the duration of the *data* period when the RN contends with other k active nodes and different

events happen in the cycle: i) when a successful frame is transmitted by the RN ($T_{d,s,k}$); ii) when a frame transmitted by the RN collides ($T_{d,f,k}$); iii) when the RN overhears a successful frame transmitted by a node different from the RN ($T_{d,os,k}$); and, iv) when the RN overhears a frame transmitted by a node different from the RN that collides ($T_{d,of,k}$). Also, $E_{aw,1} = q_{1,0} \cdot [(T - T_{sync} - T_{d,s,0}) \cdot P_{rx}] + q_{2,0} \cdot [(T - T_{sync} - (t_{RTS} + D_p + (W - 1)/2)) \cdot P_{rx}]$ and $E_{aw,0} = [(T - T_{sync} - (W + t_{RTS} + D_p)) \cdot P_{rx}]$ where $T_{d,s,0} = t_{RTS} + f_0 \cdot t_{DATA} + t_{CTS} + t_{ACK} + 4D_p + (W - 1)/2$, and $T_{d,os,0} = t_{RTS} + D_p + (W - 1)/2$. Recall that in cycles where there are not active nodes in the network, the RN has to overhear the medium during the maximum duration of the backoff time, which is W .

Similarly, the energy consumed by the RN during the *sleep* period of a normal cycle, $E_{nr,k}$, can be obtained by replacing the P_{rx} with the sleep power level, P_{sl} , in (17).

4) *Total Average Energy Consumption per Cycle*: The average energy consumed by the RN during the *data* period of a cycle is given by,

$$E_d = \sum_{k=0}^N E_{d,k} \cdot \pi'_k \quad (18)$$

where π'_k is the stationary probability of finding k active nodes in the network. For the 3D and 2D DTMCs these probabilities can be respectively determined by,

$$\pi'_k = \begin{cases} \sum_{i=1}^Q \sum_{r=0}^R \pi(i, k-1, r) + \pi(0, k, 0) & \text{for 3D} \\ \sum_{i=1}^Q \pi(i, k-1) + \pi(0, k) & \text{for 2D} \end{cases} \quad (19)$$

for $1 \leq k \leq N-1$. Also, $\pi'_0 = \pi(0, 0, 0)$ or $\pi'_0 = \pi(0, 0)$, and $\pi'_N = \sum_{i=1}^Q \sum_{r=0}^R \pi(i, N-1, r)$ or $\pi'_N = \sum_{i=1}^Q \pi(i, N-1)$, respectively.

The average energy consumed during the *sleep* period of a *normal* cycle is obtained by

$$E_{nr} = \sum_{k=0}^N E_{nr,k} \cdot \pi'_k. \quad (20)$$

The average energy consumed during the *sleep* period of a cycle belonging to an *awake* super-cycle where the node is awake is determined by

$$E_{aw} = \sum_{k=0}^N E_{aw,k} \cdot \pi'_k. \quad (21)$$

Then, the average energy consumption during the *sleep* period of a cycle is obtained by

$$E_{sl} = \frac{E_{nr} \cdot N_{sc} \cdot (N_{aw} - 1) + E_{aw} \cdot N_{sc}}{N_{sc} \cdot N_{aw}}. \quad (22)$$

Finally, the total average energy consumed by the RN in a cycle is obtained by

$$E = E_{sc} + E_d + E_{sl}. \quad (23)$$

As discussed for the computation of P_s according to (5), the accuracy of the energy terms in (18), (20) and (21) improves

with the accuracy of the distribution of active nodes in the network.

E. Energy Efficiency

We define the energy efficiency of the RN, ξ , as the ratio between the average number of bytes successfully transmitted per cycle and the total average energy consumed in that cycle. In a network where *DATA* packets have a constant size of S bytes, it can be determined as,

$$\xi = \eta \cdot S/E. \quad (24)$$

Recall that the number of packets aggregated by a node in consecutive frames changes randomly.

VI. NUMERICAL RESULTS FOR ERROR-FREE CHANNELS

In this section, we compare the performance of APT against SPT by enabling finite and infinite retransmissions with an error-free channel. The analytical results are obtained based on the developed 3D and 2D DTMC models. The simulation results are obtained by implementing the transmission schemes in a custom-built C based discrete-event simulator.

The developed simulator mimics the physical behavior of the APT and SPT schemes. That is, in each cycle a node receives packets according to a given discrete distribution, contends for channel access with other nodes if it has packets in the buffer, and, if it wins, then transmits a frame (a packet) using APT (SPT). The simulation results are completely independent of those obtained by the analytical models. That is, the calculation of the performance metrics in our simulations is not dependent on the derived mathematical expressions at all, nor are the state transition tables used in these calculations. The performance results reported below are the average values of the measurements made over $5 \cdot 10^6$ cycles and the accuracy of the models is validated later in this section.

TABLE IV
TIME PARAMETERS (UNIT: MILLISECOND)

Cycle duration (T)	60	Propagation delay (D_p)	0.001
t_{RTS} , t_{CTS} and t_{ACK}	0.18	t_{SYNC}	0.18
t_{DATA}	1.716	Contention Window (W)	128

Consider a WSN as the one illustrated in Figure 1. To investigate the performance of our models, the network is configured with the following parameters: number of sensor nodes $N \in \{5, \dots, 30\}$, queue capacity of a node $Q = 10$, *DATA* packet size is $S = 50$ bytes, the APT scheme is configured with a maximum number of packets per frame $F \in \{2, 5, 10\}$, packet arrival rate $\lambda \in [0.5, 4.5]$ packets/s, $N_{sc} = 10$, $N_{aw} = 40$, the transmission, reception and sleep power levels are: $P_{tx} = 52$ mW, $P_{rx} = 59$ mW and $P_{sl} = 3$ μ W [23], respectively. The duration of a backoff time slot is configured as 0.1 ms. The time parameters are summarized in Table IV.

We adopt the term *load* to refer to the offered traffic, i.e., the ratio between the packet arrival rate and the packet service rate. Observe that the packet arrival rate does not depend on the transmission scheme implemented by the nodes, i.e., APT or

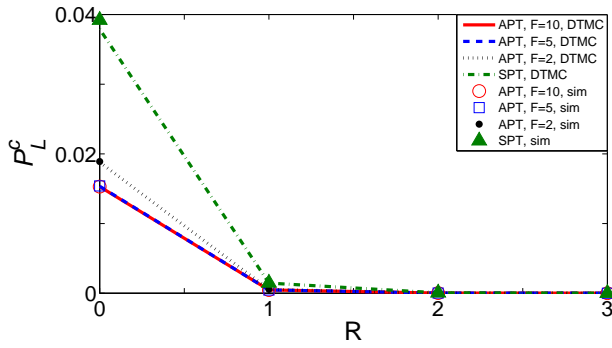


Fig. 3. Variation of the packet loss probability due to collisions, when retransmissions are enabled with $\lambda = 4.5$ packets/s and $N = 5$.

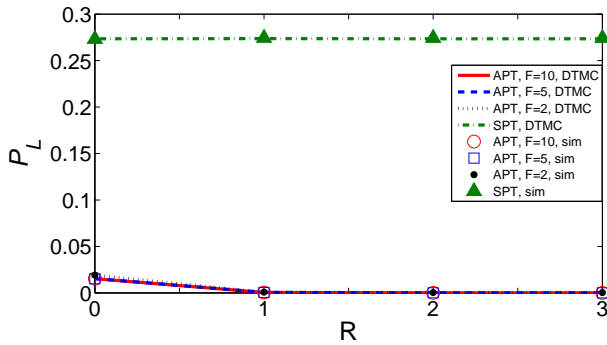


Fig. 4. Variation of the *total* packet loss probability, when retransmissions are enabled with $\lambda = 4.5$ packets/s and $N = 5$.

SPT. On the other hand, the packet service rate clearly depends on the transmission scheme as, on average, the number of packets transmitted successfully per cycle increases with F . Then, for the same arrival rate, a node, or the network, is more loaded when SPT is deployed than when APT is deployed.

A. APT versus SPT with Finite Retransmissions

Two extreme packet arrival rate conditions are investigated, that correspond to the arrival rates of $\lambda = 0.5$ (light traffic load) and 4.5 packets/s (heavy traffic load), respectively. As a reference to reflect the intensity of the load offered to a node that deploys SPT and has $R = \infty$, the packet loss probabilities due to buffer overflow induced by these two arrival rates are approximately in the order of 10^{-12} and 10^{-1} , respectively.

Clearly, the performance of the APT scheme can be better demonstrated when $\lambda = 4.5$ packets/s. For these evaluation configurations, we define a network of $N = 5$ nodes with a single sink node, and vary the maximum number of retransmissions in the set $R \in \{1, \dots, 10\}$.

1) Impact of the Maximum Number of Retransmissions:

We evaluate the impact that the maximum number of retransmissions, R , has on the total packet loss, i.e., losses due to transmissions that collide plus losses due to buffer overflows, when $\lambda = 4.5$ packets/s. Note that once a packet is accepted in the queue, it might be successfully delivered or dropped. When retransmissions are disabled, the packet is dropped after the first collision. On the other hand, when R is infinite, the

packet stays in the queue until it is delivered successfully. When finite retransmissions are enabled, the packet is dropped after R consecutive packet retransmissions that collide.

The variation of the packet loss probability due to unsuccessful retransmissions is illustrated in Figure 3. In the figure, the curves associated with “DTMC” and “sim” show the results for finite retransmissions obtained by the corresponding 3D DTMC model and simulations respectively. The same notation is adopted in the rest of the figures in this section. Note that the results for zero retransmissions are obtained using the DTMC presented in Table III, but by replacing $P_{s,k}$ with $P_{sf,k}$. The results illustrated in Figure 3 show that a vast majority of packets require at most two retransmissions using either SPT or APT. That is, the packet loss probability due to collisions is negligible for $R \geq 2$. Clearly, the delay, throughput and energy consumption will keep constant for $R \geq 2$. For brevity, these parameters are studied only for $R = \infty$.

Figure 4 shows the variation of the total packet loss probability, P_L , including losses due to packets discarded after R retransmissions, and buffer overflows, for the APT and SPT schemes. For SPT, $P_L = 27.4\%$ and this value appears to be insensitive to R . As shown in Figure 3 for SPT, when $R > 2$ the packet drops due to collisions are negligible, then all losses are caused by buffer overflow. When $R = 0$, the SPT scheme will drop packets due to collisions. However, these losses seem to be compensated by having lower buffer overflow.

On the other hand, for the APT scheme and any value of $F \geq 2$, $P_L = 1.55\%$ for $R = 0$. Observe in Figure 4 that $P_L \approx 0\%$ for $R \geq 2$ for APT. Clearly, the capability of transmitting multiple packets (a frame) per cycle contributes decisively to reduced queue occupancy, and therefore reduces buffer overflow.

B. APT versus SPT with Infinite Retransmissions

In this subsection we employ the 2D DTMC model to compare the throughput, average packet delay and average energy consumption of APT and SPT. The results are obtained based on two configurations: i) a fixed packet arrival rate of $\lambda = 1.5$ packets/s but different number of nodes $N \in \{5, \dots, 30\}$; and ii) a fixed network size of $N = 15$ but different arrival rates $\lambda \in [0.5, 4.5]$ packets/s. Since $R = \infty$ in this model, no losses occur due to collisions over the channel, i.e., $P_L^c = 0$.

1) *Total Throughput*: Figures 5 and 7 illustrate the total network throughput Th under these two configurations. In both cases, the achieved throughput increases with the number of nodes, N , or the arrival rate, λ , up to the saturation point. For the SPT scheme, the saturation points occur at $N = 11$ and $\lambda = 1.1$ packets/s, as shown in the corresponding zoomed-in sub-figure of Figures 5 and 7 respectively. In the saturation regime, all nodes have packets to send in nearly all cycles, i.e., all nodes are active in nearly all cycles. As a reference, for $N = 15$ the fraction of cycles in which a node is not active is $\pi_0 = 1.18 \cdot 10^{-2}$, while for $N = 20$ it is $\pi_0 = 7.10 \cdot 10^{-4}$.

As shown in these figures, for SPT, Th decreases slightly as N increases beyond $N = 11$. This can be explained since we expect that for $N \geq 11$ all nodes are active in all cycles.

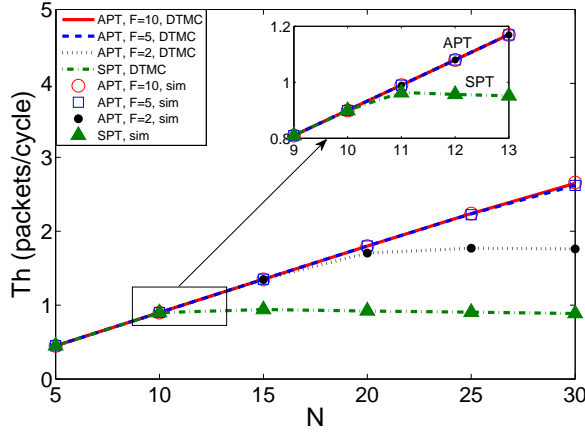


Fig. 5. Total throughput as the number of nodes varies, when $\lambda = 1.5$ packet/s and with infinite retransmissions.

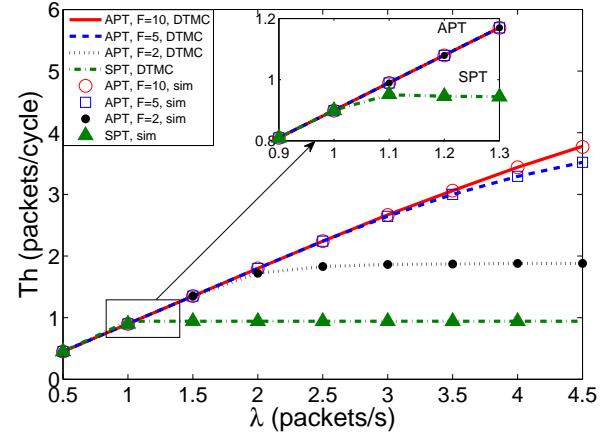


Fig. 7. Total throughput as the data arrival rate varies, when $N = 15$ and with infinite retransmissions.

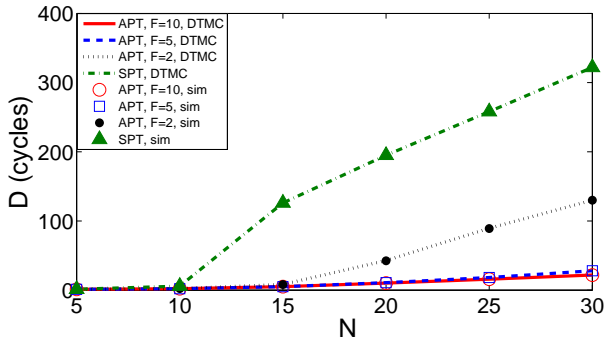


Fig. 6. Average packet delay as the number of nodes varies, when $\lambda = 1.5$ packet/s and with infinite retransmissions.

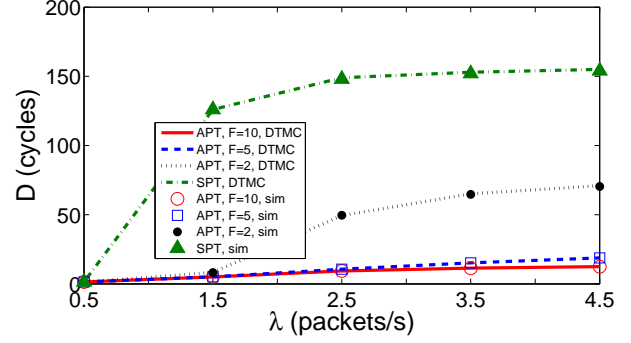


Fig. 8. Average packet delay as the data arrival rate varies, when $N = 15$ and with infinite retransmissions.

Take $N = 15$ as an example. The probability that a node transmits a packet (frame) successfully is $P_{s,14} = 0.063$, while for $N = 30$ it is $P_{s,29} = 0.030$. Recall that $P_{s,k}$ was given by (1). That is, for $N = 15$ a node achieves slightly more than 6 successful (frame) transmissions every 100 cycles, while for $N = 30$ it achieves merely 3 successful transmissions every 100 cycles, approximately. Clearly, from (11) we have that $Th(N = 30)/Th(N = 15) \approx 2P_{s,29}/P_{s,14} = 0.94$. This explains why Th decays slightly after the saturation point.

As expected, a similar trend is observed for APT, but for larger values of N as F increases. As a reference, when $F = 2$ the saturation occurs approximately at $N = 20$ and $\lambda \geq 2.5$ packets/s. Note that, once the saturation point is reached, any additional load offered to the nodes will be rejected due to buffer overflow.

2) *Average Packet Delay*: Figure 6 displays the variation of the average packet delay with the network size N and with the maximum frame size F , when $\lambda = 1.5$ packets/s. Observe that the delay is almost zero when the number of nodes is small for both the APT and the SPT schemes. The reason is that a network with a small number of nodes has little contention. Then, nodes have immediate access to the channel and can transmit packets as soon as they arrive to the queue. On the other hand, when the number of nodes increases, it

takes longer to get channel access due to increased contention. Then, packets have to wait longer time in the queue before being transmitted.

Observe the performance of SPT in Figures 5 and 6. We realize that the total throughput Th increases steadily with N up to $N = 11$, while for these network sizes the average packet delay D is very small. For $11 \leq N \leq 15$, Th does not increase but D increases sharply. We can conclude that the knee of the D and Th curves exists at $N = 11$, for the studied configuration. For $N \leq 10$, packets are transmitted as soon as they arrive at the node. Clearly, the number of active nodes per cycle is very small. However, for $N \geq 11$ collisions in the channel and delay both increase.

Figure 8 depicts the performance of the average packet delay as λ varies, for different F values, when there are $N = 15$ nodes in the network. Similar observation as discussed above applies to this scenario. The delay is almost zero for $\lambda = 0.5$, as this very low arrival rate induces very little contention in the channel. As expected, APT achieves lower average packet delay than SPT does. By simply configuring $F = 2$, a drastic delay reduction is achieved. However, increasing F beyond 5 does not seem to have any significant impact. Recall that when $F = 5$ a frame can fit as much as half of the queue capacity ($Q = 10$).

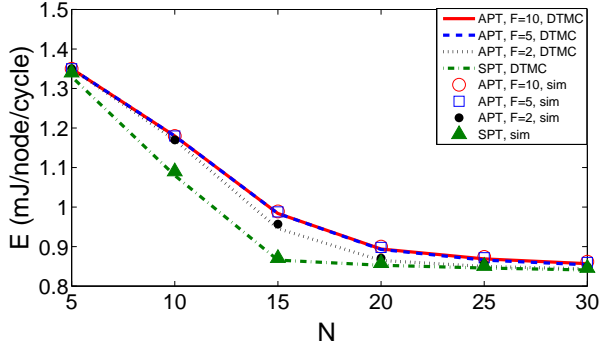


Fig. 9. Total average energy consumed by the RN as the number of nodes varies, when $\lambda = 1.5$ packet/s and with infinite retransmissions.

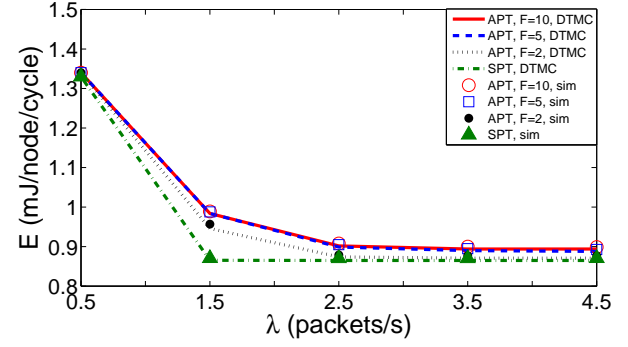


Fig. 11. Total average energy consumed by the RN as the data arrival rate varies, when $N = 15$ and with infinite retransmissions.

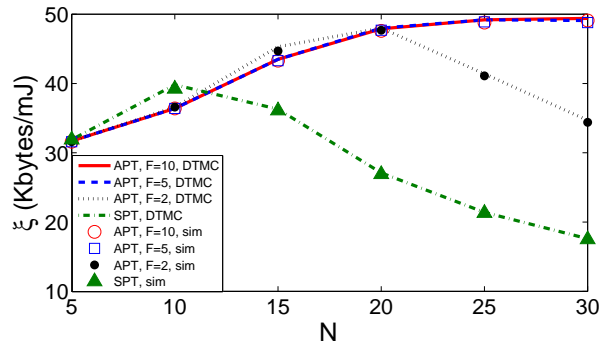


Fig. 10. Energy efficiency as the number of nodes varies, when $\lambda = 1.5$ packet/s and with infinite retransmissions.

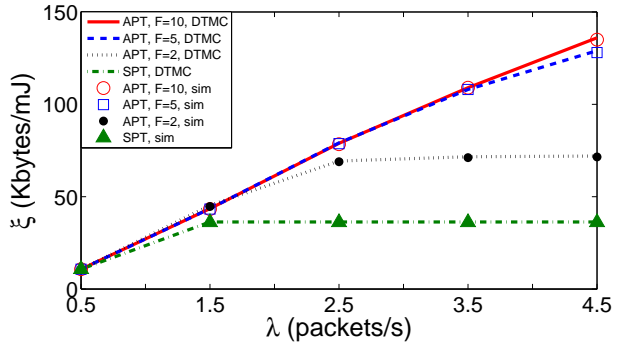


Fig. 12. Energy efficiency as the data arrival rate varies, when $N = 15$ and with infinite retransmissions.

3) *Total Average Energy Consumption:* The total average energy consumption per cycle, E , for the SPT and APT schemes is shown in Figures 9 and 11 for the two configurations studied. At a first glance it might look counter-intuitive that E is higher when the network is lightly loaded than when it is heavily loaded. This behavior is mainly due to idle listening, which is more acute in light loads. For medium and high loads, a node will go to sleep as soon as it hears an *RTS* or a collision in the channel. Whereas for light load, in many cycles nodes have to listen for the whole backoff window duration to realize that there were no active nodes.

For SPT, we observe that E decreases with the network size N and the arrival rate λ up to a point, approximately $N = 11$ and $\lambda = 1.1$ packets/s. Beyond that point, E decays approximately linearly with N or becomes constant with λ . As discussed above, at $N = 5$, the number of active nodes per cycle is very small, and then the energy consumption due to idle listening contributes significantly to E . For $N \geq 5$, E keeps on decreasing due to the increasing occupancy of the channel, up to the point ($N = 11$) beyond which the channel is busy in all cycles. The evolution of E with λ can be described in similar terms.

For APT, E behaves similarly as in SPT, but the shape of E depends now on the maximum number of packets aggregated per frame F . The total energy consumed by APT is always larger than the total energy consumed by SPT for all N and

λ values. As mentioned before, this is due to the fact that as F increases, there will be more cycles with no active nodes, and therefore more energy is wasted by overhearing in those cycles. It is worth noting that the difference between the energy consumed by the APT and SPT schemes reduces drastically as the load increases.

4) *Energy Efficiency:* Figures 10 and 12 illustrate the evolution of the energy efficiency, ξ , with the network size N and the packet arrival rate λ . As shown in the figures, the energy efficiency achieved by APT is substantially higher than the one obtained by SPT, especially at high packet arrival rates and with a large node population. For example, as shown in Figure 11, at $\lambda = 2.5$ packets/s, the total average energy consumed by a node deploying APT is only marginally higher than the one consumed by a node deploying SPT (0.39% larger for $F = 2$ and 1.65% larger for $F = 5$). On the other hand, with the same arrival rate, the total throughput Th for APT with $F = 2$, expressed as total number of packets successfully transmitted per cycle, is almost twice as much as Th for SPT, as observed in Figure 7. Note that node throughput η is equal to Th/N and the same ratio $1/N$ is maintained between Th and η for both APT and SPT.

Accordingly, for a constant packet length of $S = 50$ bytes, Figure 12 demonstrates that the energy efficiency expressed in transmitted Kbytes (per cycle and node) per consumed energy unit in mJ (per cycle and node) is almost twice as high for

APT with $F = 2$ as for SPT. A similar explanation can be formulated for the variation of the energy efficiency with the number of network nodes N .

Moreover, the evolution of ξ with N presents different maximums for different values of F , the maximum number of packets aggregated per frame. For $F = 1$ (SPT) the maximum of ξ is achieved at $N = 10$, while for $F = 2$ it is achieved at $N = 20$. Note that at these network configurations, Th achieves its maximum while D is small. This result suggests that in a network where the number of nodes varies over time and the packet arrival rate per node (λ) remains constant, an adaptive scheme that could adjust the value of F would be beneficial. This optimal F value could keep Th operating in the vicinity of its maximum while maximizing ξ and achieving low D .

When the size of the network N is fixed, the evolution of ξ with λ has a similar behavior as the evolution of Th with λ . In this case, selecting the largest possible F value for any arrival rate could achieve maximum ξ , maximum Th and minimum D . Observe that ξ for $F = 2$ is only marginally higher than ξ for $F = 5$ or 10 for $0.5 \leq \lambda \leq 1.5$. Then, selecting the largest value for F would be a very good approximation to the optimal network configuration in this arrival rate interval.

C. Accuracy of the 3D and 2D DTMC Models

In this subsection, we compare the accuracy of the results obtained by the 2D and 3D DTMC models with the results obtained by simulation for the APT and SPT schemes. The results are summarized in Table V. The configuration employed for these results is: network size $N = 20$ nodes with a single sink, queue capacity $Q = 10$ packets, and the packet arrival rate to each node $\lambda = 1.5$ packets/s.

Define the relative error of a measure as $|x - y|/y$, where x is the value obtained by the corresponding analytical model and y is the value obtained by simulation. As illustrated in Table V, the throughput and delay values obtained from the analytical models and simulations match accurately with each other, being the largest relative error 0.51% for delay in case of $F = 2$. For energy consumption, the relative error for E varies with different configurations but still lower than 0.65% in all cases. Accordingly, we conclude that the relative error of the performance parameters obtained by the analytical models is lower than 1% for all the studied parameters for both 3D and 2D DTMCs.

VII. MODELING APT IN ERROR-PRONE CHANNELS

The 2D and 3D DTMC models presented earlier in this paper were designed with an assumption that the channel was error-free. In this section, as an example of the versatility of the proposed analytical framework, we extend the 3D model to scenarios where wireless channel impairments have an impact on WSN performance.

Our models describe the WSN behavior at the MAC layer. At this layer, channel impairments are revealed via packet (frame) errors. Therefore, we aim at integrating a frame-level error model that characterizes the wireless channel condition into the 3D model. Thus a 4D model is developed. Note that

in this approach, bit error rate is neither an input parameter nor an outcome of the model.

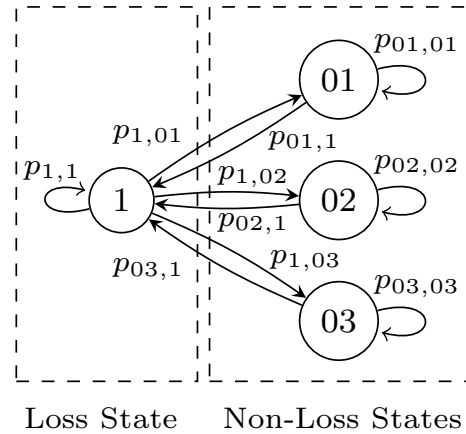


Fig. 13. A frame-level error model for error-prone channels with one state in the *loss* macro-state and three states in the *non-loss* macro-state.

A. An Extended On/Off Model for Frame-Level Errors

Different studies have proposed frame-level error models and shown that their statistical characteristics precisely match those of real packet traces [24], [25], [26]. Typically, the channel condition, with respect to the packets transmitted over it, can be regarded as either On (successful transmission) or Off (transmission failed). That is, packets transmitted without collisions while the channel is in On will be received successfully, while those transmitted while the channel is in Off will be received with errors and discarded.

The extended On/Off model proposed in [24] describes the holding times in the On and Off states by a mixture of geometric distributions. In our error model, the On and Off states are represented by two macro-states representing the *loss* and *non-loss* states respectively, where a macro-state is composed of a set of states. This modeling approach captures both first- and second-order statistics with sufficient accuracy, which is considered an adequate characterization of the wireless link for practical scenarios.

Let us represent consecutive cycles in the non-loss and loss states by a sequence of 0s and 1s, respectively. Then, a sequence of consecutive 1s represents an error burst, i.e., a set of consecutive cycles where packets (frames) transmitted will not be received successfully due to channel impairments. The mean frame error rate would be the fraction of 1s in the complete sequence.

For simplicity of configuration, we deploy a single state to describe the *loss* macro-state, and three states to represent the *non-loss* macro-state, as shown in Figure 13. This model is shown to exhibit a self-similar behavior over a finite but wide enough range of time-scales [27], and can be easily configured. The model has three parameters: H , a and b . The value of H determines the range of time-scales where the process can be considered as self-similar. Once the value of H is decided, the values of a and b are obtained such that they fit respectively the fraction of cycles where the channel produces frame-level

TABLE V
PERFORMANCE COMPARISON: SIMULATION VERSUS 3D DTMC AND 2D DTMC

Scheme	Delay (cycles)			$E(\text{mJ})$			Throughput (packets/cycle)			π_0		
	Sim	3D	2D	Sim	3D	2D	Sim	3D	2D	Sim	3D	2D
SPT	194.8	194.8	194.8	0.859	0.853	0.853	0.92	0.92	0.92	0.00	0.00	0.00
APT, $F = 2$	42.5	42.8	42.8	0.869	0.863	0.863	1.70	1.70	1.70	0.16	0.16	0.16
APT, $F = 5$	10.8	10.8	10.8	0.894	0.889	0.889	1.80	1.80	1.80	0.49	0.49	0.49
APT, $F = 10$	10.2	10.2	10.2	0.896	0.890	0.890	1.80	1.80	1.80	0.51	0.51	0.51

errors $\rho_{FE} = (1 - 1/b)/(1 - 1/b^H)$, and the average number of consecutive cycles where the channel produces frame-level errors (average error burst length) $E[B] = (\sum_{k=1}^{H-1} a^{-k})^{-1}$.

In the adopted model, we configure $H = 4$. Accordingly, we set $b = 0.4418$ to obtain a frame error rate (FER) of $\rho_{FE} = 5\%$, and $a = 2$ to obtain a mean frame-error burst length of $E[B] = 1.143$. This is a realistic configuration according to field measurements performed in [25]. However, any other values can be configured in the model.

Denote by P_{NE} the transition matrix that describes the cycles where the channel is in non-loss states. Note that P_{NE} is equal to the transition matrix that defines the 3D DTMC, and that was shown in Table II. Also, denote by P_E a new transition matrix that describes the cycles where the channel is in loss states and is shown in Table VI. Then, a new transition matrix which encompasses the transmissions in both macro states needs to be constructed.

The new transition matrix, denoted by P , has the following block structure:

$$P = \begin{bmatrix} A_0 & A_1 & A_2 & A_3 \\ B_1 & B_4 & 0 & 0 \\ B_2 & 0 & B_5 & 0 \\ B_3 & 0 & 0 & B_6 \end{bmatrix}. \quad (25)$$

where $A_0 = p_{1,1}P_E$, $A_m = p_{1,0m}P_E$, $B_m = p_{0m,1}P_{NE}$, $B_n = p_{0m,0m}P_{NE}$, and $m = 1, 2, 3$. Clearly, matrices A_0 to A_3 represent the network states in channel error-prone cycles, while matrices B_1 to B_6 describe the network states in channel error-free cycles. As defined in [27], $p_{1,1} = 1 - \sum_{k=1}^{H-1} 1/a^k$, $p_{1,0m} = 1/a^m$, $p_{0m,1} = (b/a)^m$, and $p_{0m,0m} = 1 - (b/a)^m$, where $m = 1, 2, 3$.

B. State Description of the 4D DTMC Model

In the 4D DTMC, the state vector is denoted by (i, k, r, e) , where i is the number of packets found at the queue of the RN, k keeps track of the number of active nodes in the network, r is the number of retransmissions experienced by the packet at the head of the queue of the RN, and e is a new tuple representing the channel state as presented in Figure 13. When $e = 1$ a transmitted frame will not be received correctly, whereas when $e = \{01, 02, 03\}$ the transmitted frames will be received successfully, provided that they did not collide. Note that now a transmission failure happens due to either errors in the channel or contention collision. For further details about the 4D model, like the definition of the transition matrix P and the expressions for the performance parameters, please refer to [28].

C. Numerical Result Example under the 4D Model

Based on the constructed state transition matrix P , we are able to obtain the steady state probabilities for each state. Following the same procedure as presented earlier, we deduce the closed-form expressions for the investigated performance parameters.

As an example, we illustrate in Figure 14 the total throughput under an error-free (E-F) channel and an error-prone (E-P) channel with $\text{FER} = 5\%$, obtained from both the 4D analytical model (DTMC) and simulations (sim). The network is configured as in Figure 5 where $\lambda = 1.1$ packet/s, but with $R = 10$, and N varies from 5 to 30. Again, the analytical results match with the ones obtained from simulations. It is also evident that a slightly lower throughput is achieved in the error-prone channel scenario. However, note that the decrease of Th is only marginal, as most of the frames discarded at reception due to errors induced by the channel are recovered by retransmission.

D. Brief Discussion on Model Complexity

Finally, we compare the complexity of the developed models in terms of the number of states in the DTMC models. The number of states in the 2D, 3D, and 4D DTMCs is $N \times (Q + 1)$, $N \times (Q + 1) \times (R + 1)$, and $N \times (Q + 1) \times (R + 1) \times H$ respectively. The state space cardinality of the DTMC grows very fast as N , Q , R and (or) H increases. This can render the application of simple matrix inversion procedures to determine the stationary distribution infeasible. In such systems, more elaborate iterative and direct methods have been proposed in order to obtain the stationary distribution [29]. For a simple iterative method applicable to moderately large DTMCs, please refer to [30].

VIII. CONCLUSIONS

In this paper, we have proposed an analytical model to evaluate the performance of an aggregated packet transmission (APT) scheme. It operates in WSNs with a synchronous duty-cycled MAC protocol like S-MAC. The model is based on a 3D DTMC. Unlike existing models for duty-cycled MAC protocols, our model integrates the dependence among the nodes by modeling the number of active nodes in the network. In addition, we have also developed a less complex 2D DTMC model for APT in scenarios where packet loss due to collisions in the channel is negligible, as well as a 4D model which integrates the impact of error-prone channels.

TABLE VI
TRANSITION PROBABILITIES OF THE 4D DTMC MODEL MATRIX \mathbf{P}_e IN THE LOSS STATE

No active node exists. Transitions occur due to new arrivals	
$P_{(0,0,0),(j,l,0)} = B_l(K) \cdot A_j; 0 \leq j < Q, 0 \leq l \leq K,$	$P_{(0,0,0),(Q,l,0)} = B_l(K) \cdot A_{\geq Q}; 0 \leq l \leq K.$
No packets in the queue of the RN, i.e., no transmissions by the RN. Transitions are caused by the other k active nodes	
$P_{(0,k,0),(j,l,0)} = B_{l-k}(K-k) \cdot A_j$ $0 \leq j < Q, 1 \leq k \leq l \leq K,$	$P_{(0,k,0),(Q,l,0)} = B_{l-k}(K-k) \cdot A_{\geq Q}$ $1 \leq k \leq l \leq K,$
No transmission attempt	
$P_{(i,k,r),(j,l,r)} = (1 - P_{sf,k}) \cdot B_{l-k}(K-k) \cdot A_{j-i}$ $1 \leq i \leq j < Q, 0 \leq k \leq l \leq K, 0 \leq r \leq R,$	$P_{(i,k,r),(Q,l,r)} = (1 - P_{sf,k}) \cdot B_{l-k}(K-k) \cdot A_{\geq Q-i}$ $1 \leq i \leq Q, 0 \leq k \leq l \leq K, 0 \leq r \leq R,$
Failed transmission by the RN due to channel impairments	
$P_{(i,k,r),(j,l,r+1)} = P_{sf,k} \cdot B_{l-k}(K-k) \cdot A_{j-i}$ $1 \leq i \leq j < Q, 0 \leq k \leq l \leq K, 0 \leq r < R,$	$P_{(i,k,r),(Q,l,r+1)} = P_{sf,k} \cdot B_{l-k}(K-k) \cdot A_{\geq Q-i}$ $1 \leq i \leq Q, 0 \leq k \leq l \leq K, 0 \leq r < R.$
$P_{(i,k,R),(j,l,0)} = P_{sf,k} \cdot B_{l-k}(K-k) \cdot A_{j-i+\alpha}$ $1 \leq i \leq Q, i - \alpha \leq j < Q, 0 \leq k \leq l \leq K,$	$P_{(i,k,R),(Q,l,0)} = P_{sf,k} \cdot B_{l-k}(K-k) \cdot A_{\geq Q-i+\alpha}$ $1 \leq i \leq Q, 0 \leq k \leq l \leq K.$

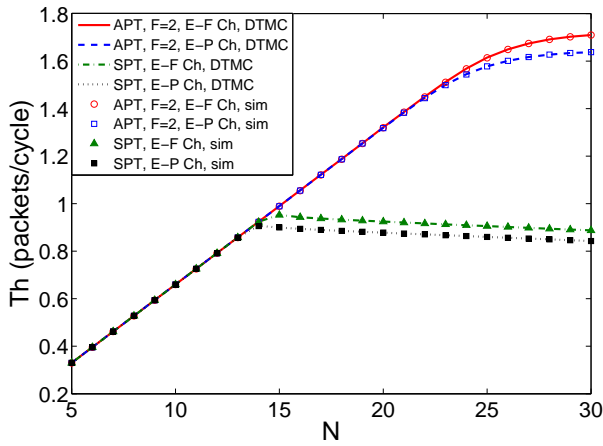


Fig. 14. Total throughput under an error-prone channel as the number of nodes varies, when $\lambda = 1.1$ packet/s, $R = 10$ and FER = 5%.

With these models, we obtain closed-form expressions for performance parameters like throughput, average packet delay, packet loss, energy consumption and energy efficiency. The analytical models are validated through extensive discrete-event based simulations. It is shown that they are very accurate, with relative errors below 1%.

The obtained analytical and simulation results show that APT outperforms its single packet transmission (SPT) counterpart in terms of packet loss, average delay and throughput, as more packets can be aggregated per transmitted frame. Therefore, migrating from SPT to APT is a natural choice when the load of the network increases. Even though the total energy consumption required for APT is slightly higher than for SPT, much higher energy efficiency is achieved in terms of the number of bytes transmitted per Joule.

REFERENCES

- [1] W. Ye, J. Heidemann, and D. Estrin, "Medium access control with coordinated adaptive sleeping for wireless sensor networks," *IEEE/ACM Trans. Netw.*, vol. 12, no. 3, pp. 493–506, Jun. 2004.
- [2] R. Rajagopalan and P. K. Varshney, "Data-aggregation techniques in wireless sensor networks: a survey," *IEEE Commun. Surveys Tuts.*, vol. 8, no. 4, pp. 48–63, 2006.
- [3] K. Akkaya, M. Demirbas, and R. S. Aygun, "The impact of data aggregation on the performance of wireless sensor networks," *Wireless Commun. Mobile Comput.*, vol. 8, no. 2, pp. 171–193, Feb. 2008.
- [4] M. Bagaa, Y. Challal, A. Ksentini, A. Derhab, and N. Badache, "Data aggregation scheduling algorithms in wireless sensor networks: Solutions and challenges," *IEEE Commun. Surveys Tuts.*, vol. 16, no. 3, pp. 1339–1368, Third Quarter 2014.
- [5] G. Bianchi, "Performance analysis of the IEEE 802.11 distributed coordination function," *IEEE J. Select. Areas Commun.*, vol. 18, no. 3, pp. 535–547, Mar. 2000.
- [6] R. P. Liu, G. J. Sutton, and I. B. Collings, "A new queuing model for QoS analysis of IEEE 802.11 DCF with finite buffer and load," *IEEE Trans. Wireless Commun.*, vol. 9, no. 8, pp. 2664–2675, Aug. 2010.
- [7] O. Yang and W. Heinzelman, "Modeling and performance analysis for duty-cycled MAC protocols in wireless sensor networks," *IEEE Trans. Mobile Comput.*, vol. 11, no. 6, pp. 905–921, Jun. 2012.
- [8] L. Dai and X. Sun, "A unified analysis of IEEE 802.11 DCF networks: Stability, throughput, and delay," *IEEE Trans. Mobile Comput.*, vol. 12, no. 8, pp. 1558–1572, 2013.
- [9] J. Luo, L. Jiang, and C. He, "Performance analysis of synchronous wakeup patterns in contention-based sensor networks using a finite queuing model," in *Proc. IEEE GLOBECOM*, 2007, pp. 1334–1338.
- [10] Y. Zhang, C. He, and L. Jiang, "Performance analysis of S-MAC protocol under unsaturated conditions," *IEEE Commun. Lett.*, vol. 12, no. 3, pp. 210–212, Mar. 2008.
- [11] O. Yang and W. Heinzelman, "Modeling and throughput analysis for S-MAC with a finite queue capacity," in *Proc. IEEE ISSNIP*, 2009, pp. 409–414.
- [12] J. Martinez-Bauset, L. Guntupalli, and F. Y. Li, "Performance analysis of synchronous duty-cycled MAC protocols," *IEEE Wireless Commun. Lett.*, vol. 4, no. 5, pp. 469–472, 2015.
- [13] F. Tong, L. Zheng, M. Ahmadi, M. Li, and J. Pan, "Modeling and analyzing duty-cycling, pipelined-scheduling MACs for linear sensor networks," *IEEE Trans. Veh. Technol.*, 2015, early access available in IEEEExplore.
- [14] S. C.-H. Huang, P.-J. Wan, C. T. Vu, Y. Li, and F. Yao, "Nearly constant approximation for data aggregation scheduling in wireless sensor network," in *Proc. IEEE INFOCOM*, 2007, pp. 366–372.
- [15] X. Xu, X. Y. Li, X. Mao, S. Tang, and S. Wang, "A delay-efficient algorithm for data aggregation in multihop wireless sensor networks," *IEEE Trans. Parallel and Distrib. Syst.*, vol. 22, no. 1, pp. 163–175, Jan. 2011.
- [16] L. Galluccio and S. Palazzo, "End-to-end delay and network lifetime analysis in a wireless sensor network performing data aggregation," in *Proc. IEEE GLOBECOM*, 2009, pp. 1–6.
- [17] B. Alinia, M. H. Hajiesmaili, and A. Khonsari, "On the construction of maximum-utility aggregation trees in deadline-constrained WSNs," in *Proc. IEEE INFOCOM*, 2015, pp. 1–9.

- [18] M. Kamarei, M. Hajimohammadi, A. Patooghy, and M. Fazeli, "An efficient data aggregation method for event-driven WSNs: A modeling and evaluation approach," *Wireless Personal Commun.*, vol. 84, pp. 745–764, 2015.
- [19] K. Nguyen, U. Meis, and Y. Ji, "An energy efficient, high throughput MAC protocol using packet aggregation," in *Proc. IEEE GLOBECOM Workshops*, 2011, pp. 1236–1240.
- [20] Z. Li, Y. Peng, D. Qiao, and W. Zhang, "Joint aggregation and MAC design to prolong sensor network lifetime," in *Proc. IEEE ICNP*, 2013, pp. 1–10.
- [21] Y. Sun, O. Gurewitz, and D. Johnson, "RI-MAC: A receiver-initiated asynchronous duty cycle MAC protocol for dynamic traffic loads in wireless sensor networks," in *Proc. ACM SenSys*, 2008, pp. 1–14.
- [22] Z. Li, Y. Peng, D. Qiao, and W. Zhang, "LBA: Lifetime balanced data aggregation in low duty cycle sensor networks," in *Proc. IEEE INFOCOM*, 2012, pp. 1844–1852.
- [23] MICA, "http://edge.rit.edu/edge/P08208/public/Controls_Files/MICaZ-DataSheet.pdf," data sheet.
- [24] P. Ji, B. Liu, D. Towsley, Z. Ge, and J. Kurose, "Modeling frame-level errors in GSM wireless channels," *Performance Evaluation*, vol. 55, no. 1, pp. 165–181, 2004.
- [25] G. Boggia, P. Camarda, and A. D'Alconzo, "Performance of Markov models for frame-level errors in IEEE 802.11 wireless LANs," *Int. J. Commun. Syst.*, vol. 22, no. 6, pp. 695–718, 2009.
- [26] D. Striccoli, G. Boggia, and A. Grieco, "A Markov model for characterizing IEEE 802.15. 4 MAC layer in noisy environments," *IEEE Trans. Indus. Electron.*, vol. 62, no. 8, pp. 5133–5142, 2015.
- [27] S. Robert and J.-Y. Le Boudec, "New models for pseudo self-similar traffic," *Performance Evaluation*, vol. 30, no. 1, pp. 57–68, 1997.
- [28] L. Guntupalli, J. Martinez-Bauset, F. Y. Li, and M. Weitnauer, "Modeling and performance evaluation of synchronous DC MAC protocols in error-prone wireless links," Technical Report. [Online]. Available: <http://personales.upv.es/jmartine/smac4d.pdf>
- [29] W. J. Stewart, *Probability, Markov Chains, Queues, and Simulation: The Mathematical Basis of Performance Modeling*. Princeton University Press, 2009.
- [30] X. Gelabert, J. Pérez-Romero, O. Sallent, and R. Agustí, "A Markovian approach to radio access technology selection in heterogeneous multi-access/multiservice wireless networks," *IEEE Trans. Mobile Comput.*, vol. 7, no. 10, pp. 1257–1270, 2008.

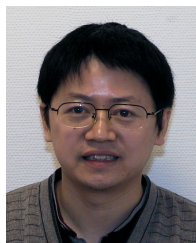


Lakshmikanth Guntupalli (S'13) received the B.Tech. degree in electronics and communications engineering from the Jawaharlal Nehru Technological University, Hyderabad, India, in 2005 and the M.E. degree in electronics and telecommunication engineering from the S. G. S. Institute of Technology and Science, Indore, India, in 2008. He is currently working toward the Ph.D. degree at the Department of Information and Communication Technology, University of Agder (UiA), Norway.

His research interests include the areas of green wireless communications, wireless sensor networks, mobile ad hoc networks and performance evaluation of communication protocols and networks.



Jorge Martinez-Bauset holds a Ph.D. from the Universitat Politècnica de València (UPV), Spain, and currently is an Associate Professor at the same university. From 1987 to 1991 he was with QPSX Communications in Perth (Western Australia), working with the team that designed the first IEEE 802.6 MAN. He has been with the Dep. of Communications of the UPV since 1991. He was recipient of the 1997's Alcatel Spain best Ph.D. thesis award in access networks. His research interests are in the area of performance evaluation and traffic control for multi-service networks. In these areas he has published a number of papers in refereed journals and conference proceedings, and has participated in different research projects sponsored by the European Commission and the Spanish government, as well as by private companies.



Frank Y. Li (S'99-M'03-SM'09) received the Ph.D. degree from the Norwegian University of Science and Technology (NTNU), Trondheim, Norway. He worked as a Senior Researcher at UniK-University Graduate Center, University of Oslo, Norway before joining the Department of Information and Communication Technology, University of Agder (UiA), Agder, Norway, in August 2007 as an Associate Professor and then a Full Professor. During the past few years, he has been an active participant in several Norwegian and EU research projects. He is

listed as a Lead Scientist by the European Commission DG RTD Unit A.03-Evaluation and Monitoring of Programmes in Nov. 2007. Dr. Li's research interests include MAC mechanisms and routing protocols in 4G and beyond mobile systems and wireless networks, mesh and ad hoc networks; wireless sensor network; D2D communication; cooperative communication; cognitive radio networks; green wireless communications; reliability in wireless networks, QoS, resource management and traffic engineering in wired and wireless IP-based networks; analysis, simulation and performance evaluation of communication protocols and networks.



Mary Ann Weitnauer (formerly Mary Ann Ingram) has been a Georgia Tech ECE faculty member for 26 years. Her early research areas were optical communications and radar. Since the mid 90's, she has focused on the application of both real and virtual antenna arrays to wireless communications, with emphasis on Layers 1 through 3 of multi-hop ad hoc, mesh, WLAN, and sensor networks. She directs the Smart Antenna Research Laboratory (SARL), which demonstrates many of its works on a 20-node network of software defined radios (SDRs) in

practical environments and topologies. SARL has also recently developed algorithms for impulse radio-ultrawideband (IR-UWB) radar, for non-contact vital signs sensing. Dr. Weitnauer has authored or co-authored over 180 refereed journal and conference papers, and received four Best Paper awards in conferences. She was an associate editor for the IEEE Transactions on Mobile Computing from 2009-2012. She was a Visiting Professor at Aalborg University, Aalborg, Denmark in the summers of 2006-2008 and at Idaho National Labs in 2010. She was the CTO for Sensiotech Inc. 2012-14. Dr. Weitnauer is a Senior Member of the IEEE.